Biogeochemistry (2012) 110:243–255
DOI 10.1007/s10533-011-9674-z

A mechanistic explanation of the Sargasso Sea DMS "summer paradox"

Luca Polimene · Stephen D. Archer · Momme Butenschön · J. Icarus Allen

Received: 14 March 2011 / Accepted: 18 October 2011 / Published online: 10 November 2011

Abstract In the Sargasso Sea, maximum dimethylsulfide (DMS) accumulation occurs in summer, concomitant with the minimum of chlorophyll and 2 months later than its precursor, dimethylsulfoniopropionate (DMSP). This phenomenon is often referred to as the DMS "summer paradox". It has been previously suggested that the main agent triggering this pattern is increasing irradiance leading to light stress-induced DMS release from phytoplankton cells. We have developed a new model describing DMS(P) dynamics in the water column and used it to investigate how and to what extent processes other than light induced DMS exudation from phytoplankton, may contribute to the DMS summer paradox. To do this, we have conceptually divided the DMS "summer paradox" into two components: (1) the temporal decoupling between chlorophyll and DMSP and (2) the temporal decoupling between DMSP and DMS. Our results suggest that it is possible to explain the above cited patterns by means of two different dynamics, respectively: (1) a succession of phytoplankton types in the surface water and (2) the bacterially mediated DMSP(d) to DMS conversion, seasonally varying as a function of nutrient limitation. This work differs from previous modelling studies in that the presented model suggests that phytoplankton light-stress induced processes may only partially explain the summer paradox, not being able to explain the decoupling between DMSP and DMS, which is possibly the more challenging aspect of this phenomenon. Our study, therefore, provides an "alternative" explanation to the summer paradox further underlining the major role that bacteria potentially play in DMS production and fate.

Keywords DMSP · DMS · Marine ecosystem models · DMS summer paradox

L. Polimene (✉) · S. D. Archer · M. Butenschön · J. I. Allen
Plymouth Marine Laboratory, Prospect Place, The Hoe, Plymouth PL1 3DH, UK
e-mail: luca@pml.ac.uk

Introduction and background

Dimethylsulfide (DMS) is a volatile organic sulphur compound which accounts for more than 50% of the global natural sulphur flux to the atmosphere (Liss et al. 1997). The fate of DMS in the atmosphere is complex, but can directly contribute to new aerosol particle production and cloud condensation nuclei, potentially moderating cloud albedo and climate (e.g. Charlson et al. 1987). DMS is a product of bacterial- or phytoplanktonic-mediated enzymatic cleavage of the S-containing osmolyte, β-dimethylsulphoniopropionate (DMSP), synthesised by a variety of phytoplankton (Keller et al. 1989). However, in most cases, DMS concentrations cannot be confidently predicted from phytoplankton biomass, taxonomic composition or even

DMSP concentrations. For example, a temporal decoupling between maximum concentrations of chlorophyll, DMS and DMSP was observed in seasonal studies in subtropical and temperate latitudes (Dacey et al. 1998; Vila-Costa et al. 2008; Archer et al. 2009). Difficulty in explaining this apparently widespread phenomenon has led some authors to define it as the DMS "summer paradox' (Simó and Pedrós-Alió 1999).

Recent modelling studies (Le Clainche et al. 2010; Vallina et al. 2008; Toole et al. 2008) explained the DMS summer accumulation observed at Hydrostation-S (Dacey et al. 1998), close to the Bermuda Atlantic Time-series Study station (BATS) in the Sargasso Sea, by assuming a direct exudation of DMS by phytoplankton dictated by elevated ultraviolet irradiance during summer months. This interpretation is based on a putative antioxidant role for DMSP and its breakdown products that may be up-regulated by phytoplankton in high irradiance, low nutrient surface waters and may result in the release of DMS directly from cells (Sunda et al. 2002). However, the above cited models, whilst properly simulating the average DMS concentration, and/or the temporal decoupling between chlorophyll and DMSP, do not explain the separation by 2 months of the monthly averaged, water-column integrated, maximum concentrations of particulate DMSP and DMS observed over the 3 year period at Hydrostation-S. This suggests that other processes could be involved in the evolution of this pattern (Simo and Pedros Alio' 1999; Vogt et al. 2010).

In this study, we developed a new model describing DMS(P) dynamics in the water column to test how and to what extent processes different from phytoplankton light induced DMS exudation contribute to the evolution of the summer paradox. In particular we test the hypothesis that a phytoplankton type succession might explain the decoupling between chlorophyll and DMSP and that the bacteria mediated DMSPd to DMS conversion might explain the decoupling between DMSP and DMS.

The formulation of the DMS(P) dynamics is embedded in the simplified version of the ERSEM model (Blackford et al. 2004) described in Fig. 1a. ERSEM was coupled with the General Ocean Turbulence Model (GOTM, Burchard et al. 1999), a 1D water column model which dynamically simulates the evolution of temperature, density and vertical mixing when forced with metrological data. The GOTM–ERSEM coupled model was implemented at BATS (31° 40′ N, 64° 10′ W), resolving the first 250 m of the water column. The model is forced with reanalysis meteorological data (ECMWF) for the vicinity of the BATS site and initialised with temperature, salinity and nutrient concentrations observed in situ. At the lower boundary of the water column a simple remineralisation closure is applied exporting sinking detritus that is re-injected into the water column as dissolved nutrients and inorganic carbon at a fixed rate of 0.5 day^{-1} (Fig. 1a).

Sulphur-containing compounds are modelled through their molar carbon component (sulphur is not explicitly modelled). However, DMSP, DMSPd and DMS are converted into units of sulphur for diagnostic purposes.

Simulations have been run for 5 years (1990–1994) of which the last three (1992–94) were analysed, compared with observations and discussed.

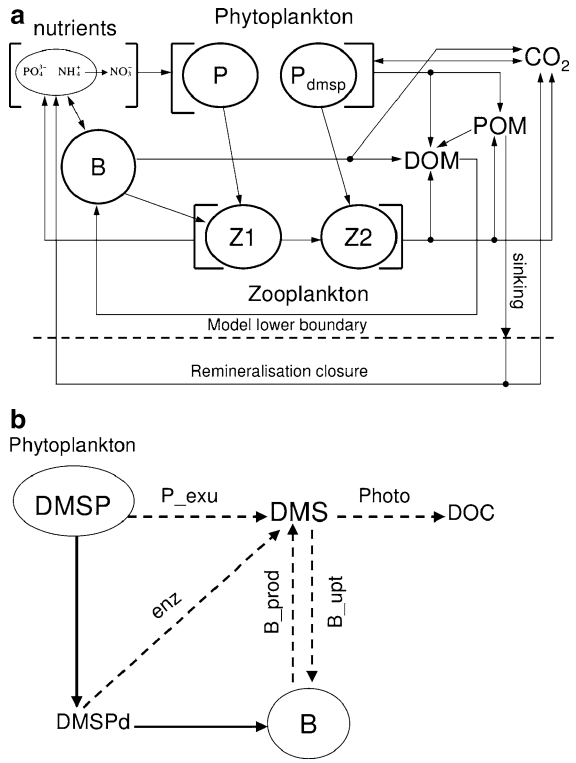

Fig. 1 Modelled food web (**a**) and modelled DMS(P) biogeochemical fluxes (**b**). *P and* P_{dmsp} Phytoplankton functional types, *Z1 and Z2* zooplankton functional types, *B* bacteria functional type, *DOM* dissolved organic matter, *POM* particulate organic matter, *DOC* dissolved organic carbon. *Dashed arrows* in panel **b** refer to the processes described in Eq. 4 and are labelled accordingly

The DMS–ERSEM model

The ERSEM model is extensively described in Blackford et al. (2004) and we refer the reader to that paper for a full description of the ERSEM structure and underlying philosophy. We limit our description to the DMS(P) formulation and to any parts of the model which has been modified with respect to Blackford et al. (2004). In Table 1, the parameters relating to the DMS(P) formulations and those that have been changed with respect to Blackford et al. (2004) are reported. The modelled DMS(P) biogeochemical fluxes are shown in Fig. 1b.

Plankton functional types

The model trophic structure is composed of two phytoplankton, two zooplankton and one bacterial functional type (Fig. 1a). Phytoplankton is conceptually divided in two types (P and P_{dmsp}) differing from each other primarily through their capacity to produce DMSP. Type P is able to produce only a small

Table 1 Model parameters

Parameter	Units	Value	Reference
P Max photosynthetic rate (r)	day^{-1}	3.3	This study
P Max Chl:C (ϑ_{max})	mg Chl mg C^{-1}	0.075	This study
P Min DMSP:C (DP_{min})	mol C g C^{-1}	0.00167	This study
P Max DMSP:C (DP_{max})	mol C g C^{-1}	0.00167	This study
P Affinity for NH_4^a	$(mg\ C)^{-1}\ day^{-1}$	0.05	This study
P Affinity for PO_4^a	$(mg\ C)^{-1}\ day^{-1}$	0.005	This study
P_{dmsp} Max photosynthetic rate (r)	day^{-1}	1.5	This study
P_{dmsp} Max Chl:C (ϑ_{max})	mg Chl mg C^{-1}	0.03	This study
P_{dmsp} Min DMSP:C (DP_{min})	mol C g C^{-1}	0.00167	This study
P_{dmsp} Max DMSP:C (DP_{max})	mol C g C^{-1}	0.0167	This study
P_{dmsp} Affinity for NH_4^a	$(mg\ C)^{-1}\ day^{-1}$	0.01	This study
P_{dmsp} Affinity for PO_4^a	$(mg\ C)^{-1}\ day^{-1}$	0.0025	This study
P_{dmsp} DMS exudation rate (λ^{exu})	d^{-1}	0.1	This study
Irradiance threshold level (I_{max})	W m^{-2}	80	Vogt et al. (2010)
DMS:DMSPd carbon molar ratio (ξ)	mol C mol C^{-1}	0.4	
Z1 lower threshold for feeding	mg C m^{-3}	2.5	This study
Z2 lower threshold for feeding	mg C m^{-3}	2	This study
Z2 assimilation rate at 10°C	d^{-1}	1.5	This study
P1 relative availability for Z1	adim	0.6	This study
P2 relative availability for Z1	adim	0	This study
P1 relative availability for Z2	adim	0	This study
P2 relative availability for Z2	adim	0.4	This study
B1 relative availability for Z1	adim	0.7	This study
B1 relative availability for Z2	adim	0	This study
Z1 relative availability for Z2	adim	0.5	This study
Z1 relative availability for Z1	adim	0.2	This study
Z2 relative availability for Z2	adim	0.2	This study
Bac. optimal P cellular quota (p^{opt})	mol P g C^{-1}	0.0019	Polimene et al. (2006)
Bac. optimal N cellular quota (n^{opt})	mol N g C^{-1}	0.017	Polimene et al. (2006)

P and P_{dmsp} are treated as P3 and P4 in Blackford et al. (2004), respectively, apart from the parameters above specified. Z1 and Z2 are treated as Z5 and Z4 in Blackford et al. (2004) respectively, apart from the above described parameters

[a] See Blackford et al. (2004) for the nutrient uptake formulation

(constant) amount of DMSP while type P_{dmsp} is able to increase the DMSP cellular level in response to increasing light, in accordance with the DMSP antioxidant hypothesis proposed by Sunda et al. (2002). As explained in the next paragraph, our formulation implies that a high DMSP cellular quota enables a better photosynthetic rate under high light regimes (i.e. surface layer and/or summer period) providing also a parameterisation of the DMSP cellular function as an antioxidant/photoprotective compound. P and P_{dmsp} also differ in their maximum photosynthetic rate (r), maximum chlorophyll to carbon ratio (ϑ_{max}) and affinity for nutrients (see table 1). Zooplankton is modelled by two functional types, Z1 and Z2. Z1 is specialized to feed on P and bacteria, while Z2 feeds on P_{dmsp} and Z1.

In accordance with the standard ERSEM framework, heterotrophic bacteria are described by means of only one functional group.

DMSP and DMSPd production

The daily DMSP production is assumed to be formed by two additive terms: the first is a fixed minimum carbon quota (DP_{min}) of the net primary production (NPP) i.e. the minimum fraction of NPP converted to DMSP. The second term, consistently with the antioxidant hypothesis (Sunda et al. 2002), is an enhancement function (>0) dependant on light-induced stress and is constrained by the maximum theoretically achievable DMSP cellular quota (DP_{max}). The equation for DMSP is therefore written as:

$$\frac{\partial DMSP}{\partial t} = NPP \cdot DP_{min} + (1 - E) \cdot (DP_{max} - DP) \cdot P \cdot \nu - R \cdot DMSP \quad (1)$$

where P is the phytoplankton biomass; ν is the inverse time scale of the process (1/day), DP is the dynamic DMSP to carbon ratio and R is the sum of all the loss processes (exudation, lysis and grazing). E represents the light induced stress level and is given by the ratio between the saturating parameter for photosynthesis and the incoming amount of irradiance I:

$$E = \min\left(1, \frac{Ir}{I}\right) \quad (2)$$

with Ir being the photosynthesis saturation parameter (Geider et al. 1997) modified in order to include the DMSP photo-protective function:

$$Ir = \frac{r}{\alpha \cdot \vartheta_{max}} \cdot \frac{DP}{DP_{min}} \quad (3)$$

where r is the maximum photosynthetic rate, α is the initial, chlorophyll specific, slope of the production/irradiance curve and $\vartheta_{max}$is the maximum chlorophyll to carbon ratio.

The gross primary production, formulated following Geider et al. (1997), is scaled by E, consequently, when I is higher than Ir, a decrease of the photosynthetic rate is predicted by the model.

DMSPd is considered to be a fraction (depending on the DMSP cellular quota) of the dissolved organic carbon (DOC) produced via nutrient stress-driven exudation, cell lysis and grazing (Blackford et al. 2004).

DMS sources and sinks

DMS dynamics are described through the following terms: phytoplankton exudation (P-exu) bacterial DMSPd to DMS conversion (B-prod), bacterial consumption (B-upt), free enzymes activity (enz) and photolysis (photo) (Fig. 1b):

$$\frac{\partial DMS}{\partial t} = \left.\frac{\partial DMS}{\partial t}\right|^{P-exu} + \left.\frac{\partial DMS}{\partial t}\right|^{B-prod} + \left.\frac{\partial DMS}{\partial t}\right|^{enz} - \left.\frac{\partial DMS}{\partial t}\right|^{B-upt} - \left.\frac{\partial DMS}{\partial t}\right|^{photo} \quad (4)$$

Phytoplankton DMS production (P-exu)

DMS exudation in the model is described as being dependent on the incoming irradiance and on nutrient deficiency. Based on the evidence that nutrient limitation may strongly enhance the release of DMS (Sunda et al. 2007), a term describing the cellular nutrient deficiency has been combined with the formulation proposed by Vogt et al. (2010) which assumes the process to be dependent only on light:

$$\frac{\partial DMS}{\partial t} = \lambda_{exu} \cdot DMSP \cdot \xi \cdot \max\left[(1 - N_{lim}), \frac{I}{I_{max}}\right] \quad (5)$$

where λ_{exu} is the exudation rate, ξ is the molar carbon quota of DMSP exuded as DMS (i.e. DMS:DMSPd given as carbon molar ratio), $I_{max}$is the irradiance threshold for exudation and $N_{lim}$is the ERSEM nutrient limitation parameter described in Blackford

et al. (2004). N_{lim} varies from 0 and 1 with maximal limitation for values close to zero.

Bacterial DMSPd and DMS consumption (B-upt) and DMS production (B-prod)

The dynamics of the standard ERSEM bacteria submodel have been updated with the formulation proposed by Polimene et al. (2006) assuming active exudation of semi-labile carbon and nutrient uptake/remineralisation to equilibrate the internal stoichiometry. Organic matter uptake and production is conceptually described as in Polimene et al. (2006). However, we decided to not include the processes describing the release of bacteria capsular material (Stoderegger and Herndl 1998) and the resulting production of recalcitrant "semi-refractory" organic carbon as these processes are not relevant to this work. Both DMSPd and DMS are treated as a part of the labile dissolved organic carbon pool (LDOC). However, different turnover rates have been consistently observed for the two compounds, 0.6 to 1.5 day^{-1} and 0.1 to 0.2 day^{-1} for DMSPd and DMS, respectively (Malmstrom et al. 2004; Bailey et al. 2008). Consequently, we assume a bacterial degradation time scale of 1 day for DMSPd and 5 days for DMS. The uptake of DMSPd and DMS is proportional to the relative quota of these compounds within the dissolved organic matter pool.

Bacterial-mediated DMS production from DMSPd is assumed to be modulated by the bacterial nutritional status (Kiene et al. 2000) in the following way:

$$\frac{\partial \mathrm{DMS}}{\partial t} = \mathrm{DMSP_{upt}} \cdot \xi \cdot \max\left[0,\ \max\left(1 - \frac{\mathrm{qpb}}{\mathrm{p^{opt}}},\ 1 - \frac{\mathrm{qnb}}{\mathrm{n^{opt}}}\right)\right] \quad (6)$$

where $DMSP_{upt}$ is the DMSPd uptake, ξ is the molar carbon quota of DMSPd transformed into DMS, qpb and qnb are the varying cellular phosphorus and nitrogen (relative to carbon) and p^{opt} and n^{opt} are the "optimal" phosphorus and nitrogen to carbon ratios (Polimene et al. 2006).

Free enzymes activity and photolysis

The contribution of free enzyme activity to DMSPd cleavage generating DMS and DMS photo-oxidation have been formulated as in Archer et al. (2004). DMS generated by free enzymes is then described by a constant DMSPd cleavage rate (assumed to be 0.01 day^{-1}) while a simplistic Michaelis–Menten formulation based on irradiance is used to describe DMS photo-oxidation.

Other DMS source and loss processes

Given the focused goals of this study all other processes accounting for DMS production and/or loss (sea-to-air flux, grazing and viral lysis of phytoplankton), which are thought to be not directly involved in the evolution of the DMS "summer paradox", are not considered in the current model implementation.

Results and discussion

General physical and biological conditions

Simulated temperature, phosphate and chlorophyll yearly (1992–94) averaged values in the form of 2 dimensional (Hovmoller) diagrams are shown in Fig. 2. The simulations reproduce the main general features of the BATS ecosystem such as the seasonal thermal stratification and the summer deep chlorophyll maximum layer between 80 and 100 m depth (Steinberg et al. 2001). The largest vertical mixing is simulated in March when temperature is homogeneous from the surface down to 200 m depth, while, starting from June, a strong thermal stratification is simulated by the model.

Simulated phosphate is generally low in the surface layer (<0.03 μM) increasing only in the deeper part of the water column where (between 100 and 150 m) the model depicts a steep nutricline. However, during the winter thermal mixing, the model simulates a breakdown of the nutricline with relatively high amounts of phosphate reaching the surface layer in spring. Conversely, minimal PO_4 values are simulated in summer concomitant with the thermal stratification. This weak PO_4 surface seasonality plays (as will be better explained later) an important role in our modelling interpretation of the DMS summer paradox. As both model and observed PO_4 concentrations (Steinberg et al. 2001) are very close to the detection limits (~0.01 μM), it is difficult to make a meaningful quantitative comparison between the two. We can argue that upwelled nutrients are rapidly taken-up by

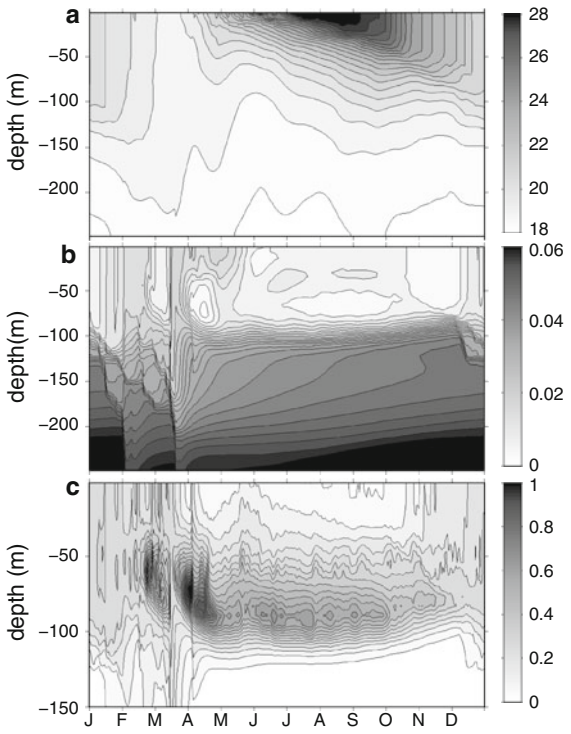

Fig. 2 Average temporal evolution of simulated **a** temperature (°C) **b** PO_4 (mmol m^{-3}) and **c** chlorophyll (mg m^{-3}) profiles (1992–1994). Contour intervals are 0.5 (°C), 0.002 (mmol m^{-3}) and 0.05 (mg m^{-3}), respectively

phytoplankton and/or bacteria, resulting in PO_4 surface concentrations close to or below the analytical detection limit throughout the year. However, the PO_4 surface seasonal dynamics simulated by the model, can be realistically explained on the basis of the observed seasonality of surface primary production and chlorophyll (both with maxima in winter) and from the fact that, in winter-spring, the mixed layer depth is considerably deeper than the nutricline (Steinberg et al. 2001), implying a significant nutrient supply to the surface layer.

A comparison between, monthly averaged depth-integrated (0–140 and 0–40 m), observed and simulated primary and bacterial production is shown in Fig. 3. Observed primary production estimated with the ^{14}C-methodology is compared with the modelled gross (GPP), net (NPP) and particulate (pPP) primary production. We define pPP as the organic carbon produced by phytoplankton less the loss due to DOC exudation which, in ERSEM (Baretta et al. 1995; Blackford et al. 2004), is primarily a function of nutrient limitation (which does not affect the CO_2 uptake directly). Consequently, the fact that pPP is the only version of PP which qualitatively captures the pattern of the observed seasonality (with maximum in winter), suggests it may be driven by nutrient availability. However, pPP tends to underestimate the data especially the maximum observed in March, while both modelled NPP and GPP are closer to the observed values. Simulated bacteria production is in reasonable agreement with the observation in terms of both amount and seasonal cycle for the 140 m integrated values while the model tends to overestimate the 40 m integrated values observed in winter. Overall these results indicate that the simulated values of both phytoplankton and bacteria production, although with some discrepancies with respect to the observations, are not unrealistic.

The average temporal evolution of the simulated DMSP, DMSPd and DMS profiles are displayed in Fig. 4. DMSP and DMS are in reasonable agreement with the values reported in the literature for the Sargasso Sea (Dacey et al. 1998; Vallina et al. 2008) with DMSP and DMS maximal values of 15–20 and 4–6 nM, respectively, simulated in spring–summer in the upper part of the water column, between 0 and 40 m. In contrast, simulated DMSPd, with maximal values of 7–10 nM, is overestimated as observed maximal values at BATS fall between 3 and 5 nM (Vallina et al. 2008). The possible reasons for this overestimation and its implication will be discussed later.

The DMS "summer paradox"

A direct comparison between simulated monthly mean, depth integrated chlorophyll, DMSP and DMS and relative observations is offered in Fig. 5. Chlorophyll concentrations were measured in samples collected monthly at BATS (31° 40′ N, 64° 10′ W) in the Northern Sargasso Sea, (http://bats.bios.edu), while DMSP, and DMS were measured biweekly in samples from Hydrostation-S (31° 40′ N, 64° 10′ W) 50 km NW of BATS (Dacey et al. 1998). As the highest DMS concentrations are generally observed between 20 and 35 m (Dacey et al. 1998), the analysis focuses on the top 40 m of the water column. The data depict the DMS summer paradox showing the maximum of chlorophyll in February, the maximum of DMSP in May, and the maximum of DMS 2 months later, in July. The model chlorophyll reproduces the general

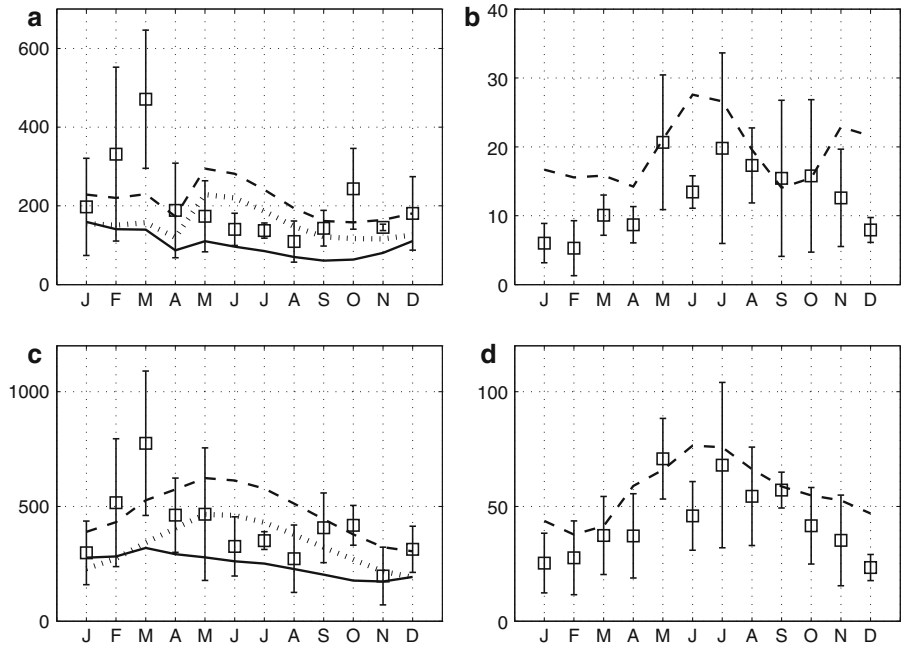

Fig. 3 Simulated and observed, monthly averaged, depth integrated primary (**a** and **c**) and bacterial (**b** and **d**) production (1992–1994). Panels **a** and **b** refer to 0–40 m integrated values while **c** and **d** refer to 0–140 m integrated values. In panels **a** and **c** primary production measured with the ^{14}C technique (*squares*) is compared with the model gross (*dashed line*), net (*dotted line*) and particulate primary production (*continuous line*), see text for details. In panels **b** and **d** observed (*squares*) and modelled (*dashed line*) bacterial production are compared. Observations are displayed with standard deviations. Units are mg C m^{-2} day^{-1}

trend in the observations, peaking in winter with minimum values in summer, although with an overestimation of chlorophyll at the beginning of summer.

The general temporal evolution of DMSP and DMS is captured by the model, albeit with maximal values of DMS simulated in June instead of July. However, although reduced from 1 to 2 month, the model still simulates a time lag between DMSP and DMS maxima, which from a modelling point of view, is the most challenging aspect of the DMS summer paradox.

Temporal decoupling between DMSP and DMS

The simulations shown until now have been our reference simulation (REF), which considers both phytoplankton and bacterial mediated processes as sources of DMS. As our hypothesis is that bacteria play the main role in the decoupling between DMSP and DMS, it is crucial to assess the relative contribution of the bacterial DMS production to that from phytoplankton exudation. In order to do this, a sensitivity experiment has been carried out by switching "on" and "off" the two processes. Hereafter we refer to simulation 1 (SIM1) when the bacteria DMS production is considered as the only DMS source and to simulation 2 (SIM2) when phytoplankton exudation is assumed to be the only DMS source. We also increased the temporal resolution of our analysis considering daily averaged simulations and focussing on the May–August period. Results relative to DMS are reported in Fig. 6. DMSP is not reported because it does not vary in SIM1 and SIM2 with respect to the reference simulation peaking in all the cases at year day 149. In SIM1, the model reproduces the maximum degree of decoupling between DMSP maximum and DMS maximum, with DMS peaking at day 192 (Fig. 6). However, the rate of DMS increase varies, showing an earlier relative maximum at day 149. As will be better explained later, this is due to the relatively fast changes in bacterial stoichiometry which affects bacteria sulphur demand at temporal scales lower than a month.

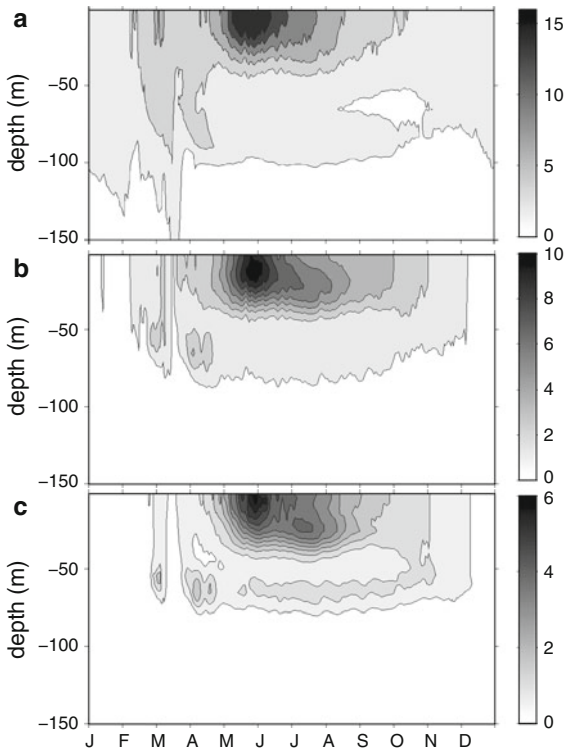

Fig. 4 Average temporal evolution of simulated **a** DMSP, **b** DMSPd and **c** DMS profiles (1992–1994). Contour intervals are 2, 1 and 0.5, respectively. Units are µmol S m^{-3}

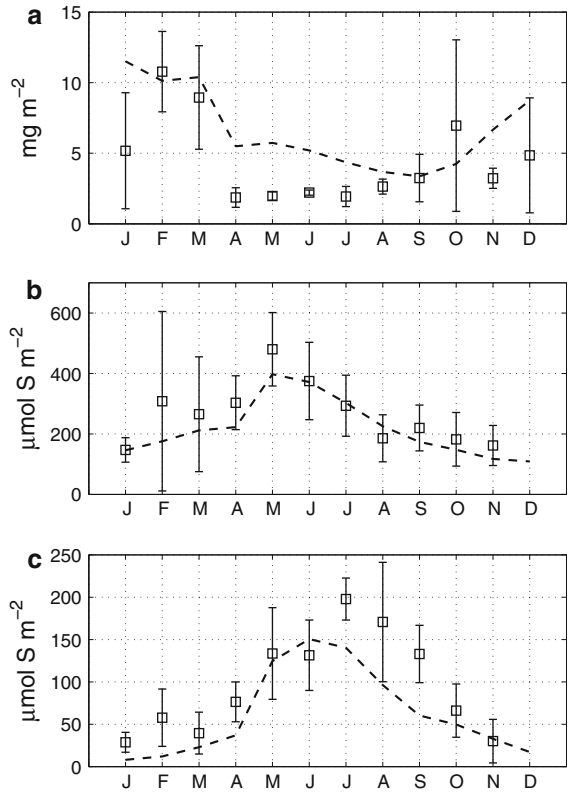

Fig. 5 Monthly mean, depth integrated (0–40 m) simulated (*dashed line*) and observed (*squares*) **a** Chlorophyll, **b** DMSP and **c** DMS temporal evolution (1992–1994). Observed mean values are displayed with standard deviation

In SIM2, the decoupling decrease from 40 to 2 days as DMS peaks at day 151. The same temporal decoupling of 2 days occurs in the reference simulation. The decoupling does not change if alternative formulations describing DMS exudation are considered: specifically, we also assumed phytoplankton DMS production to be dependent on light only (Vogt et al. 2010; Vallina et al. 2008) or only on nutrient deficiency (Fig. 6). Based on these results, the model suggests that bacterial DMS production (SIM1), modelled according to the hypothesis proposed by Kiene et al. (2000), is the only process which, qualitatively, is able to reproduce a temporal decoupling between DMSP and DMS which is comparable with observations. In fact, when SIM1 is displayed as monthly averaged values (Fig. 7) the temporal lag between simulated DMSP and DMS is 2 months (DMSP peaks in May while DMS peaks in July) in agreement with the observations (see Fig. 5).

The determination index (R^2) between observed (monthly averaged) DMS values and those for SIM1, SIM2 and the reference simulation are shown in Table 2. The determination index is a measure of the co-variance of two datasets (in our case between observed and simulated values), providing a qualitative view of the agreement between observation and simulations. R^2 is higher in SIM1, it decreases slightly in the reference simulation and shows the lowest value in SIM2. This implies that SIM1 depicts a DMS temporal trend which better captures the "shape" of the observations. The low slope (Fig. 8) for SIM1 denotes that simulated DMS strongly underestimates the observations. This underestimation tends to be less dramatic in SIM2 and in the reference simulation. This behaviour is also confirmed by the root mean square error (RMSE) values also shown in Table 2. The RMSE is an objective measurement of the distance (in terms of amount) between data and simulations with lower values indicating the closest distance (best fit). The RMSE (here normalized to the mean of the observations) is highest in SIM1 and decreases in

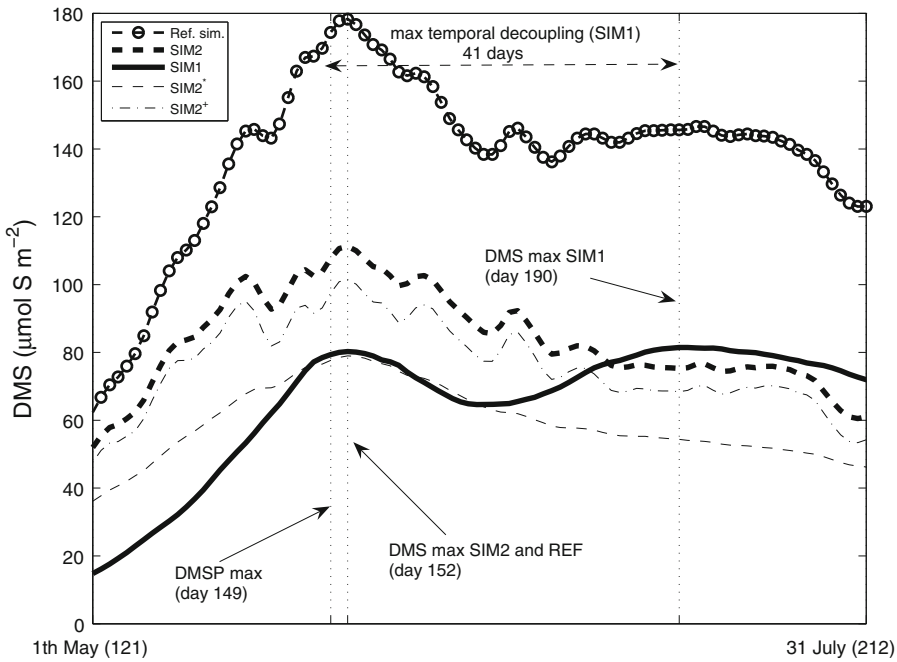

Fig. 6 Simulated daily mean, depth integrated (0–40 m) DMS in SIM1, SIM2 and the reference simulation. Figure refers to the average period from May to July (1992–1994). On the X axis are displayed the year day numbers. $SIM2^{*}$ = as SIM2 but with DMS exudation assumed to be dependent on nutrient stress only. $SIM2^{+}$= as SIM2 but with DMS phytoplankton exudation assumed to be dependent on irradiance only

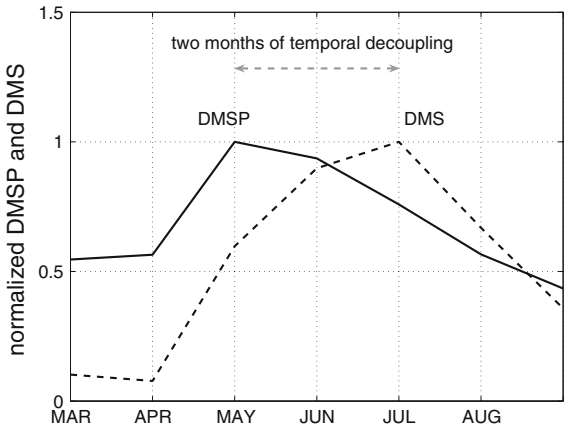

Fig. 7 Simulated, monthly averaged, depth integrated (0–40 m) DMSP (*continuous line*) and DMS (*dashed line*) concentrations in SIM1 normalized to the respective maximal values. (1992–1994)

SIM2 and in the reference simulation. Combining the two statistical indices used (R^2 and RMSE), it is clear that the reference simulation, which accounts for both the DMS production processes, is the modelling setup which, on average, best reproduces the observations. Furthermore, and most importantly for our purposes, the model suggests that phytoplankton-mediated production contributes mainly to DMS background levels and is coupled to the substrate DMSP, while the bacterial-mediated production is the process that

Table 2 RMSE and R^2 values relative to observed and simulated depth (0–40 m) integrated, monthly means, DMS concentrations

	SIM1	SIM2	REF simulation
RMSE	0.83	0.75	0.54
R^2 ($P < 0.001$)	0.56	0.43	0.55

RMSE has been normalized to the mean of the observations

drives the decoupling between DMS and DMSP. This is confirmed by the simulated bacterial- and phytoplankton-mediated DMS production in the reference simulation (Fig. 9). The maximum simulated bacterial DMS production occurs in July, while the maximum phytoplankton DMS production occurs in May, concomitant with the maximum in DMSP. The relative contribution of phytoplankton-mediated DMS production to the total DMS production tends to decrease in late summer when bacteria are dominant (Fig. 11).

DMS bacterial production as described by Kiene et al. (2000) has been considered in previous modelling studies describing DMS dynamics (Vallina et al. 2008; Bopp et al. 2008). However, in contrast to these previous studies which describe bacteria using implicit formulation (Bopp et al. 2008) or by implying fixed cellular stoichiometry (Vallina et al. 2008), we describe bacterial dynamics by modelling carbon, nitrogen and phosphorus content of bacteria

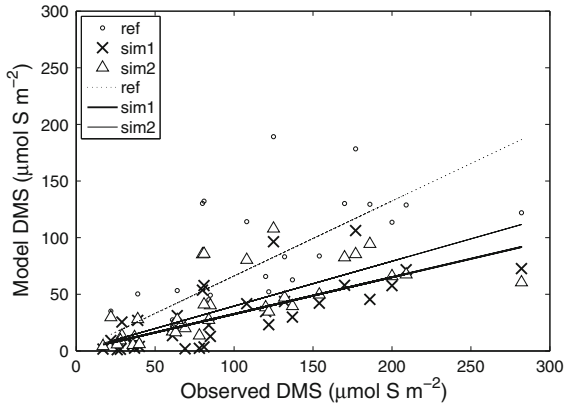

Fig. 8 Scatter plot between observed and simulated, monthly averaged, depth integrated (0–40 m) DMS in SIM1, SIM2 and the reference simulation. In figure are also displayed the regression lines

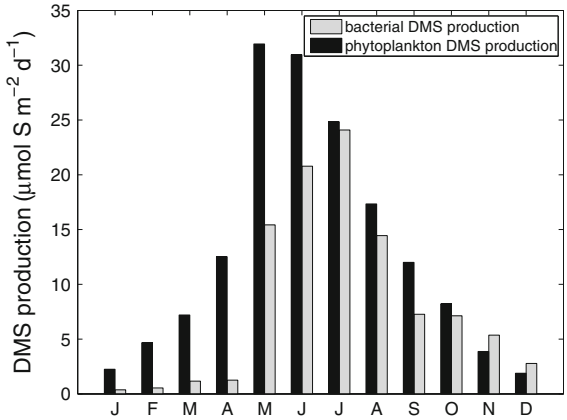

Fig. 9 Simulated, monthly averaged, depth integrated (0–40 m) phytoplankton and bacteria mediated DMS production (reference simulation)

independently. Following the formulation proposed by Polimene et al. (2006) bacteria are assumed to regulate their internal stoichiometry by actively releasing semilabile DOC and/or by remineralising or taking-up dissolved nutrients. Consequently, under sub-optimal nutrient concentrations (nutrient limitation) bacteria release surplus carbon, while, under supra-optimal nutrient concentrations (carbon limitation), they remineralise the nitrogen and phosphorous in excess. In the same way, assuming sulphur demand to be inversely proportional to nutrient limitation, bacteria fully assimilate DMSPd under carbon limited conditions whilst releasing part of it as DMS under

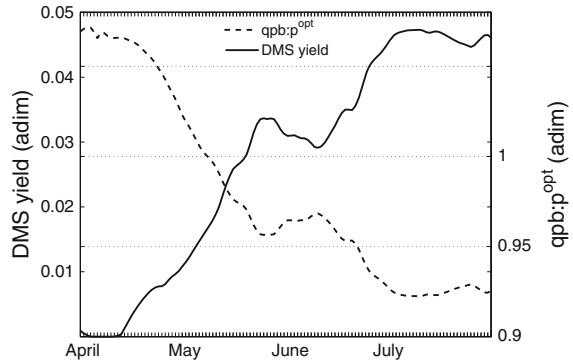

Fig. 10 Simulated daily averaged bacterial DMS production yield and (*continuous line*) model ratio between the actual (qpb) and the optimal (p^{opt}) bacterial nutrient quota (*dashed line*)

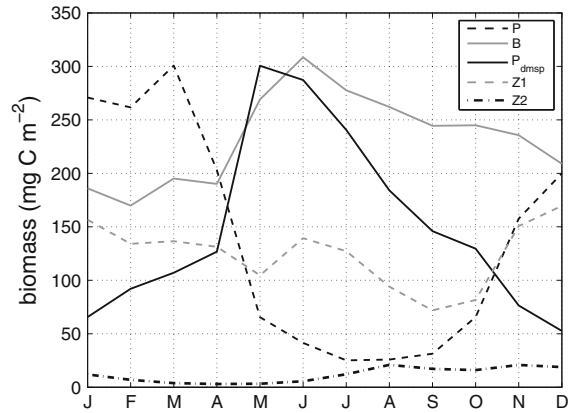

Fig. 11 Simulated, monthly averaged, temporal evolution of the depth integrated (0–40 m) biomass of the plankton functional types described by the model (1992–1994)

nutrient limited conditions. In this latter case, the DMS production yield from metabolised DMSP increases in proportion to the severity of the limitation. This "modelling interpretation" of the Kiene et al. (2000) hypothesis is shown in Fig. 10. The model ratio between qpb and p^{opt} describes the bacterial nutritional status: when its values are greater than 1, bacteria are growing in a carbon limited context, while, values lower than 1, imply a nutrient limited condition. Starting from April–May the model simulates an increase in nutrient limitation which, in turn, increases the DMS bacterial production yield. Note that the rise of the qpb to p^{opt} ratio simulated in June corresponds to the slight decrease in DMS concentration and DMS bacterial production yield simulated in the same period. This also corresponds to a peak in

zooplankton biomass (Fig. 11) which by producing nutrient-rich organic matter through grazing, allows bacteria to partially re-equilibrate their stoichiometry, temporarily increasing bacterial sulphur demand. For this reason, at a time scale of less than a month, the bacterial DMS production yield (and DMS concentration) does not increase monotonically. However, a clear seasonal shift for bacteria from nutrient replete to nutrient limited condition is depicted by the model and we regard this as the key factor driving the DMS summer paradox. Bacterial nutritional status mainly depends on the nutrient content of the DOM pool produced by phytoplankton which, in turn, is a function of inorganic nutrient availability. Inorganic nutrient supply to the surface layer is therefore considered here to be the main physical forcing, along with irradiance, which governs the DMS summer paradox. In contrast to previous modelling studies (Vallina et al. 2008; Toole et al. 2008; LeClanche et al. 2010), our results indicate that DMS(P) processes related to irradiance (DMSP production and phytoplankton DMS exudation) may only partially explain the DMS summer paradox, not being able to trigger the temporal decoupling between DMSP and DMS.

It is important to note at this point that the model, whilst underlining the importance of bacteria-mediated DMS production, could strongly underestimate the amplitude of the processes. In fact, whilst showing a clear seasonal increase, the model simulates relatively low (up to 5%, Fig. 10) values of bacterial DMS production yield. This aspect, along with the strong DMSPd overestimation (Fig. 4) suggests that DMSPd uptake and the relative release of DMS could be much faster than the time scales resolved in the model (from 1 day upwards) (Vila-Costa et al. 2006) and future model developments should take this into account.

Temporal decoupling between chlorophyll and DMSP

Phytoplankton species succession has previously been proposed as a contributing mechanism to the DMS summer accumulation (Simó and Pedrós-Alió 1999; Vallina et al. 2008), but has not been explicitly considered in many of the previous modelling studies (Lefévre et al. 2002, Vallina et al. 2008; Toole et al. 2008). Our formulation allows discrimination between PFTs not only on the basis of the cellular content of DMSP but also, and more importantly, on the basis of the antioxidant capacity that DMSP potentially provides to the phytoplankton (Sunda et al. 2002). As a consequence, the incoming irradiance drives a clear phytoplankton type succession in the upper water column, with type P (with high chlorophyll and low DMSP) dominant in winter spring and type P_{dmsp} dominant in summer (Fig. 11). This process, therefore, may potentially account for the temporal decoupling between chlorophyll and DMSP. Type P is responsible for the chlorophyll maximum in late winter while P_{dmsp} is responsible for the DMSP maximum in late spring (May). It should be stressed that the coarse, conceptual, phytoplankton classification presented is suitable for the extremely focused purposes of this study but is not meant to describe the far more complex phytoplankton community composition observed at BATS (Steinberg et al. 2001) which is outside the scope of this work.

The involvement of species succession in the formation of the DMS summer paradox has also been criticized by Toole and Siegel (2004) who stated that, during the summer, the BATS phytoplankton community is dominated by non-DMSP producing species, thus excluding the involvement of phytoplankton community succession in the DMS summer paradox evolution. It should be noted that the summer dominance of DMSP-rich phytoplankton (P_{dmsp}), simulated by our model (Fig. 11), is limited to the surface layers while the DMSP-poor phytoplankton (P) dominate throughout the year if the euphotic zone integrated values are considered (Fig. 12). This suggests that the relative importance of high DMSP-

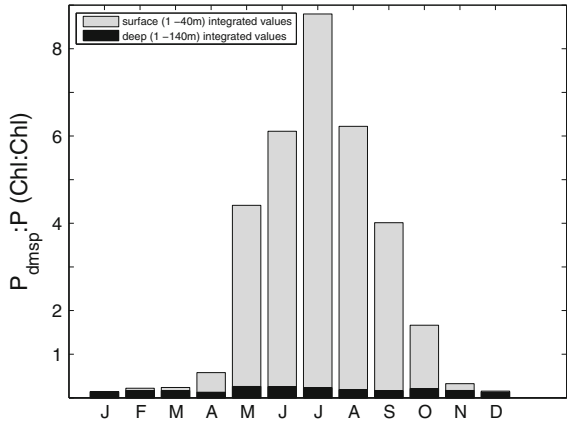

Fig. 12 Simulated, monthly averaged (1992–1994), ratio between the chlorophyll content of the two phytoplankton types (P and P_{dmsp}) described in the model. Simulated values were integrated over the 0–40 and 0–140 m depth intervals

producing phytoplanktonic species in the upper mixed layer may have been obscured in analysis based on water column integrated measurements or on data sampled in the deep chlorophyll maximum layer (Steinberg et al. 2001).

Additional modelling experiments and comparison with data are required to further validate the robustness of the proposed formulations beyond the specific environment of the Sargasso Sea. The next step would be, therefore, to implement the model in locations characterized by different trophic and light regimes that exhibit varied patterns and temporal scales of DMS and DMSP dynamics. This will help to assess if and to what extent the proposed mechanisms (phytoplankton types succession and bacteria nutrient limitation) are of relevance to modelling DMS(P) dynamics also at the global scale.

Summary and conclusion

The presented model suggests that the dynamics governing the DMS summer paradox are the result of a wide ecosystem response to seasonally changing environmental conditions. We have shown that it is possible to theoretically explain the observed temporal decoupling between maximal chlorophyll and DMSP values assuming a phytoplankton functional type succession in the upper water column (0–40 m), and to simulate the DMS summer accumulation assuming both phytoplankton and bacteria-mediated DMS production. Of these two processes phytoplankton DMS exudation strongly contributes to the amount of DMS produced, being the main DMS source for most of the year, while the bacterial-mediated DMS production is the pivotal process triggering the temporal decoupling between DMSP and DMS.

Acknowledgments This work was supported by the Natural Environment Research Council of the United Kingdom and forms part of the Surface Ocean Lower Atmosphere Studies (SOLAS) thematic projects: NE/E011314/1 (DUST-UP) and NE/C51715X/1.

References

Archer SD, Gilbert FJ, Allen JI, Blackford JC, Nightingale PD (2004) Modelling of the seasonal patterns of dimethylsulphide production and fate during 1989 at a site in the North Sea. Can J Fish Aquat Sci 61:765–787

Archer SD, Cummings DG, Llewellyn CA, Fishwick JR (2009) Phytoplankton taxa, irradiance and nutrient availability determine the seasonal cycle of DMSP in temperate shelf seas. Mar Ecol Prog Ser 394:111–124

Bailey KE, Toole DA, Blomquist B, Najjar RG, Huebert B, Kieber DJ, Kiene RP, Matrai P, Westby GR, del Valle DA (2008) Estimation of dimethylsulfide production in Sargasso Sea Eddies. Deep Sea Res II 55:1491–1504

Baretta JW, Ebenhoh W, Ruardij P (1995) The European regional Seas Ecosystem Model, a complex marine ecosystem model. Neth J Sea Res 33:233–246

Blackford JC, Allen JI, Gilbert FJ (2004) Ecosystem dynamics at six contrasting sites: a generic modelling study. J Mar Syst 52:191–215

Bopp L, Aumont O, Belviso S, Blain S (2008) Modelling the effect of iron fertilization on dimethylsulphide emission in the Southern Ocean. Deep Sea Res II 55:901–912

Burchard H, Bolding K, Villareal M (1999) GOTM: a general ocean turbulence model. Theory, applications and test cases. Technical Report EUR 18745 EN, European Commission

Charlson RJ, Lovelock JE, Andreae MO, Warren SG (1987) Oceanic phytoplankton, atmospheric sulphur, cloud albedo and climate. Nature 326:655–661

Dacey JWH, Howse FA, Michaels AF, Wakeham SG (1998) Temporal variability of dimethylsulfide and dimethylsulfoniopropionate in the Sargasso Sea. Deep Sea Res I 45: 2085–2104

Geider RJ, MacIntyre H, Kana TM (1997) Dynamic model of phytoplankton growth and acclimation: responses of the balanced growth rate and the chlorophyll a: carbon ratio to light, nutrient-limitation and temperature. Mar Ecol Prog Ser 148:187–200

Keller MD, Bellows WK, Guillard RRL (1989) Dimethyl sulfide production in marine-phytoplankton. Am Chem Soc Symp Ser 393:167–182

Kiene RP, Linn LJ, Bruton JA (2000) New and important roles for DMSP in marine microbial communities. J Sea Res 43:209–224

Le Clainche Y, Vézina A, Levasseur M, Cropp RA et al (2010) A first appraisal of prognostic ocean DMS models and prospects for their use in climate models. Global Biogeochem Cycles 24 GB3021. doi:10.1029/2009GB003721

Lefévre M, Vézina A, Levasseur M, Dacey JWH (2002) A model of dimethylsulfide dynamics for the subtropical North Atlantic. Deep Sea Res I 49:2221–2239

Liss PS, Hatton AD, Malin G, Nightingale PD, Turner SM (1997) Marine sulphur emission. Phil Trans R Soc B Biol Sci 352:159–168

Malmstrom RR, Kiene RP, Kirchman DL (2004) Identification and enumeration of bacteria assimilating dimethylsulfoniopropionate (DMSP) in the North Atlantic and Gulf of Mexico. Limnol Oceanogr 49(2):597–606

Polimene L, Allen JI, Zavatarelli M (2006) Model of interactions between dissolved organic carbon and bacteria in marine systems. Aquat Microbial Ecol 43:127–138

Simó R, Pedrós-Alió C (1999) Role of vertical mixing in controlling the oceanic production of dimethyl sulphide. Nature 402:396–399

Steinberg KS, Carlson CA, Bates NR, Johonson RJ, Michaels AF, Knap AH (2001) Overview of the US JGOFS Bermuda

Atlantic Time-series Study (BATS): a decade-scale look at ocean biology and biogeochemistry. Deep Sea Res II 48: 1405–1447

Stoderegger K, Herndl GJ (1998) Production and release of bacterial capsular material and its subsequent utilization by marine bacterioplankton. Limnol Oceanogr 43(5):877–884

Sunda W, Kieber DJ, Kiene RP, Huntsman S (2002) An antioxidant function for DMSP and DMS in marine algae. Nature 418:317–320

Sunda W, Hardison R, Kiene RP, Bucciarelli E, Harada H (2007) The effect of nitrogen limitation on cellular DMSP and DMS release in marine phytoplankton: climate feedback implication. Aquat Sci 69:341–351

Toole DA, Siegel DA (2004) Light-driven cycling of dimethylsulfide (DMS) in the Sargasso Sea: closing the loop. Geophys Res Lett 31:L09308. doi:10.1029/2004GL019581

Toole DA, Siegel DA, Doney SC (2008) A light-driven, one-dimensional dimethylsulfide biogeochemical cycling model for the Sargasso Sea. J. Geophys. Res 113:G02009. doi:10.1029/2007JG000426

Vallina SM, Simó R, Anderson TR, Gabric A, Cropp R, Pacheco JM (2008) A dynamic model of oceanic sulphur (DMSO) applied to the Sargasso Sea: simulating the dimethylsulfide (DMS) summer paradox. J Geophys Res 113:G01009. doi:10.1029/2007JG000415

Vila-Costa M, del Valle DA, Gonzales JM, Slezak D, Kiene RP, Sanchez O, Simó R (2006) Phylogenetic identification and metabolism of marine dimethylsulfide-consuming bacteria. Environ Microbiol 8(12):2189–2200

Vila-Costa M, Kiene RP, Simó R (2008) Seasonal variability of the dynamics of dimethylated sulfur compounds in a coastal northwest Mediterranean site. Limnol Oceanogr 53(1):198–211

Vogt M, Vallina SM, Buitenhuis ET, Bopp L, Le Quere C (2010) Simulating dimethylsulphide seasonality with the dynamic green ocean Model PlankTOM5. J Geophys Res 115:C06021. doi:10.1029/2009JC005529